The Journal of Immunology

Discovery and Pharmacological Characterization of a Novel Rodent-Active CCR2 Antagonist, INCB3344

Carrie M. Brodmerkel, Reid Huber, Maryanne Covington, Sharon Diamond, Leslie Hall, Robert Collins, Lynn Leffet, Karen Gallagher, Patricia Feldman, Paul Collier, Mark Stow, Xiaomei Gu, Frederic Baribaud, Niu Shin, Beth Thomas, Tim Burn, Greg Hollis, Swamy Yeleswaram, Kim Solomon, Steve Friedman, Anlai Wang, Chu Biao Xue, Robert C. Newton, Peggy Scherle and Kris Vaddi

J Immunol 2005; 175:5370-5378; ;
doi: 10.4049/jimmunol.175.8.5370
http://www.jimmunol.org/content/175/8/5370

The Journal of Immunology is published twice each month by
The American Association of Immunologists, Inc.,
1451 Rockville Pike, Suite 650, Rockville, MD 20852

Print ISSN: 0022-1767 Online ISSN: 1550-6606.

Discovery and Pharmacological Characterization of a Novel Rodent-Active CCR2 Antagonist, INCB3344

Carrie M. Brodmerkel, Reid Huber, Maryanne Covington, Sharon Diamond, Leslie Hall, Robert Collins, Lynn Leffet, Karen Gallagher, Patricia Feldman, Paul Collier, Mark Stow, Xiaomei Gu, Frederic Baribaud, Niu Shin, Beth Thomas, Tim Burn, Greg Hollis, Swamy Yeleswaram, Kim Solomon, Steve Friedman, Anlai Wang, Chu Biao Xue, Robert C. Newton, Peggy Scherle, and Kris Vaddi[1]

This report describes the characterization of INCB3344, a novel, potent and selective small molecule antagonist of the mouse CCR2 receptor. The lack of rodent cross-reactivity inherent in the small molecule CCR2 antagonists discovered to date has precluded pharmacological studies of antagonists of this receptor and its therapeutic relevance. In vitro, INCB3344 inhibits the binding of CCL2 to mouse monocytes with nanomolar potency (IC_{50} = 10 nM) and displays dose-dependent inhibition of CCL2-mediated functional responses such as ERK phosphorylation and chemotaxis with similar potency. Against a panel of G protein-coupled receptors that includes other CC chemokine receptors, INCB3344 is at least 100-fold selective for CCR2. INCB3344 possesses good oral bioavailability and systemic exposure in rodents that allows in vivo pharmacological studies. INCB3344 treatment results in a dose-dependent inhibition of macrophage influx in a mouse model of delayed-type hypersensitivity. The histopathological analysis of tissues from the delayed-type hypersensitivity model demonstrates that inhibition of CCR2 leads to a substantial reduction in tissue inflammation, suggesting that macrophages play an orchestrating role in immune-based inflammatory reactions. These results led to the investigation of INCB3344 in inflammatory disease models. We demonstrate that therapeutic dosing of INCB3344 significantly reduces disease in mice subjected to experimental autoimmune encephalomyelitis, a model of multiple sclerosis, as well as a rat model of inflammatory arthritis. In summary, we present the first report on the pharmacological characterization of a selective, potent and rodent-active small molecule CCR2 antagonist. These data support targeting this receptor for the treatment of chronic inflammatory diseases. ***The Journal of Immunology,*** **2005, 175: 5370–5378.**

Inflammatory macrophages, derived from peripheral blood monocytes, are well-characterized cell mediators of tissue destruction in a variety of chronic inflammatory diseases (1). Macrophages orchestrate tissue destruction by secreting proinflammatory cytokines such as TNF-α and IL-1β, tissue degrading enzymes such as matrix metalloproteinases, and chemokines (CXCL8, CCL5, and CCL2) that mediate the influx of other inflammatory cells. In diseases such as rheumatoid arthritis (RA),[2] disease progression correlates with the macrophage burden of the hyperplastic synovial tissue. Interestingly, response to therapies in RA often correlates with the reduction of synovial macrophages but not of other inflammatory cells (2, 3), suggesting that inhibition of monocyte migration into inflammatory lesions might be an effective mechanism to modulate disease progression in chronic inflammation.

CCR2 is a chemokine receptor predominantly expressed on monocytes that is thought to be the key receptor in mediating their tissue influx in the context of immune-based inflammation. CCR2 is a G protein-coupled receptor (GPCR), the ligands for which include the MCP family of chemokines (CCL2, CCL7, CCL8, etc.). These ligands bind CCR2 with high affinity (K_d of ~1 nM) and elicit a chemotactic signal that results in directed migration of the receptor-bearing cells. CCL2 has been shown to be present in high concentrations in various inflammatory lesions (4), implicating this chemokine as a physiologically important chemotactic signal for monocytes.

The critical role of CCL2-CCR2 as a modulator of the tissue influx of monocytes has been demonstrated most elegantly in studies of mice engineered to be deficient in either CCR2 or CCL2. Mice deficient in the receptor, CCR2, or the ligand, CCL2, whereas phenotypically normal, show a selective defect in the migration of macrophages to sites of inflammation (5–8). When subjected to disease induction, both CCR2 and CCL2 knockout mice are protected from inflammatory diseases, including experimental autoimmune encephalomyelitis (EAE; a mouse model for multiple sclerosis) (9, 10), neuropathic pain (11), and atherosclerosis (12, 13). Although these results clearly implicate CCR2 in the pathogenesis of macrophage-mediated inflammatory disorders, studies in knockout mice are inherently limited by the inability to exclude the impact of constitutive loss of CCR2 during development. In addition, CCR2 and CCL2 knockout mice have been shown to have immune perturbations that are associated with decreased IFN-γ production and decreased Th1 responses in CCR2 knockout mice (5) and with decreased Th2 responses in CCL2 knockout mice (8). Although most of the well-characterized animal models of inflammation depend on the generation of a systemic immune

Incyte Corporation, Wilmington, DE 19880

Received for publication April 20, 2005. Accepted for publication August 2, 2005.

The costs of publication of this article were defrayed in part by the payment of page charges. This article must therefore be hereby marked *advertisement* in accordance with 18 U.S.C. Section 1734 solely to indicate this fact.

[1] Address correspondence and reprint requests to Dr. Kris Vaddi, Incyte Corporation, Building 400, Route 141 and Henry Clay Road, Wilmington, DE 19880. E-mail address: kvaddi@incyte.com

[2] Abbreviations used in this paper: RA, rheumatoid arthritis; GPCR, G protein-coupled receptor; EAE, experimental autoimmune encephalomyelitis; AIA, adjuvant-induced arthritis; RT, room temperature; DTH, delayed-type hypersensitivity; DNFB, 2,4-dinitro-fluorobenzene; MOG, myelin oligodendrocyte glycoprotein; qPCR, quantitative real-time PCR.

0022-1767/05/$02.00

response to Ag, it could be argued that the protection observed in knockout mice is mainly attributable to the perturbation of the activating immune events and does not reflect true modulation of an ongoing inflammatory disease. The relevance of CCL2/CCR2 antagonism in an ongoing inflammatory disease is therefore currently unknown.

Studies using pharmacological agents can therefore provide valuable information regarding the potential therapeutic benefits of acute CCR2 inhibition in the adult. A protein antagonist of CCR2 generated by N-terminal truncation of the first 7 aas of CCL2, referred to as 7ND (14), has been used to try to determine the impact of therapeutic intervention with a CCR2 antagonist in animal models of inflammatory disease (15, 16). However, such biological agents typically have very short half-lives in blood, and the degree of inhibition required for the biological effect was never determined with this reagent. There have been no reports describing the pharmacological activity of a small molecule CCR2 antagonist in the literature. Despite a number of new compounds being disclosed as CCR2 receptor antagonists (17), virtually all of these molecules are specific for the human receptor and show little to no cross-reactivity to rodent CCR2, precluding their pharmacological evaluation in rodent models.

In this report we describe the in vitro and in vivo pharmacological characterization of INCB3344, a potent and selective rodent-active CCR2 antagonist. INCB3344 was discovered through structure-activity relationship studies based on results from a variety of in vitro binding and functional assays using a mouse cell line expressing native CCR2. INCB3344 inhibits CCL2 binding and functional responses with nanomolar potency. In vivo, INCB3344 inhibits macrophage influx and is efficacious in EAE in a manner similar to that described in $CCR2^{-/-}$ mice (9, 18). More importantly, we illustrate that therapeutic dosing of this compound results in significant efficacy in EAE as well as in the rat adjuvant-induced arthritis (AIA) model. These results demonstrate that small molecule antagonism of CCR2 both reproduces the phenotype of $CCR2^{-/-}$ mice and offers a way to evaluate the therapeutic potential of CCR2 antagonism in the variety of disease states in which macrophages are implicated.

Materials and Methods

INCB3344

INCB3344 is a small molecule antagonist (MW 577.6) of the chemokine receptor, CCR2, selected from >1000 analogs using structure-activity relationship studies determined from murine binding and chemotaxis assays (19).

Receptor binding assays

WEHI 274.1 (murine monocytic cell line; American Type Culture Collection) cells were used in a whole cell binding assay. Cells (5×10^5) in RPMI 1640 (VWR), + 0.1% BSA (Sigma-Aldrich) + 20 mM HEPES (VWR), were added to various concentrations of INCB3344 in RPMI 1640 followed immediately by the addition of 150 pM ^{125}I-labeled mCCL2 (mouse CCL2(JE)) (PerkinElmer) and incubated for 30 min at room temperature (RT). For the nonspecific control, 0.3 μM mCCL2 (R&D Systems) was added in place of INCB3344. Cells were then harvested through 1.2-μm polyvinylidene difluoride filters (Millipore), the filters were air-dried, and binding was determined by counting in a gamma counter (PerkinElmer). Antagonist activity is reported as the inhibitor concentration required for IC_{50} of specific binding. Specific binding is defined as the total binding minus the nonspecific binding and typically represents 97% of the total binding.

For the CCR5 receptor binding assay, stable transfectants of murine CCR5 were generated by using full-length mCCR5 cDNA amplified by PCR from a mouse spleen cDNA library (Clontech Laboratories). CCR5 was cloned into the mammalian expression vector, pFLAG-CMV (Sigma-Aldrich), sequenced, and transfected into HEK293SFM cells (Invitrogen Life Technologies) with Lipofectamine 2000 (Invitrogen Life Technologies). A mixed stable population was established after selection with 1000 μg/ml G-418 for 2 weeks. Mouse CCR5 expression on the cells was confirmed by FACS analysis using FACSCalibur (BD Biosciences) with the anti-FLAG M2 mAb (Sigma-Aldrich). The binding assay was performed in a 96-well MultiScreen filter plate (Millipore). The mouse CCR5 HEK293SFM transfectants (1×10^5 cells/well) in RPMI 1640 (Invitrogen Life Technologies) with 20 mM HEPES (Invitrogen Life Technologies) and 0.3% BSA (Sigma-Aldrich) were incubated at RT for 1 h with 0.2 nM ^{125}I-human MIP-1β (PerkinElmer) and a series of concentrations of either mouse MIP-1β (R&D Systems) or INCB3344. Nonspecific binding was determined by incubating the cells with 0.3 μM mouse MIP-1β (R&D Systems). Binding was determined as described above for the mCCL2-binding assay.

Chemotaxis assay

The chemotaxis assay was performed as described previously (20). WEHI-274.1 cells (5×10^5) in RPMI 1640 (VWR) with or without various concentrations of INCB3344 in RPMI 1640 were loaded in the wells on top of an 8-μm polycarbonate filter in a 96-well-modified Boyden chamber (NeuroProbe). Beneath the filter, 30 nM mCCL2 (R&D Systems) with or without INCB3344 or media was placed in a corresponding 96-well plate. The sealed chambers were incubated for 45 min at 37°C, 5% CO2. Filters were washed, stained with Wright-Giemsa (Sigma-Aldrich), and the number of cells that migrated toward mCCL2 in the bottom chamber counted by microscopy. The ability of INCB3344 to antagonize CCR2-mediated chemotaxis is reported as the inhibitor concentration required for IC_{50} values of specific migration to mCCL2. Specific migration is defined as the total migration minus the background migration. A similar assay was used to determine the impact of INCB3344 on CCR1-mediated chemotaxis of WEHI-274.1 cells, by using mouse MIP-1α (R&D Systems) as a ligand. In addition C5a, FMLP (Sigma-Aldrich) and RANTES (R&D Systems) were similarly tested in the presence of INCB3344 for migration of WEHI-274.1 cells. For the studies on the impact of INCB3344 on CCR5-mediated chemotaxis, murine T cells were used as the cell system with mouse MIP-1β as the ligand. These cells were isolated from normal mouse spleen and were cultured in RPMI 1640 media containing 10% FBS, 1× Pen/Strep, 0.1 mM nonessential amino acids, 2 mM L-glutamine, 50 μM 2-ME (all reagents from VWR), 10 ng/ml murine IL-12 (R&D Systems), and 10 μg/ml anti-murine IL-4 (BD Biosciences). Cells were placed in anti-murine CD3ϵ (BD Biosciences)-coated flasks (coated with 10 μg/ml at RT for 2 h)) for 2 days at 37°C, 5% CO2. Cells were washed with RPMI 1640 media twice and placed in fresh media with the addition of 20 ng/ml murine IL-2 (Sigma-Aldrich) in an uncoated flask for 1 day. Cells were washed twice again in RPMI 1640, and 4×10^5 cells with or without various concentrations of INCB3344 were loaded on the top of a 3-μm polycarbonate filter on a 96-well ChemoTX system plate (NeuroProbe). Beneath the filter, 30 nM murine MIP-1β (R&D Systems) with or without INCB3344, or media was placed in a corresponding 96-well plate. The plates were incubated for 2.5 h at 37°C, 5% CO2. Media in the bottom well was mixed and collected in 5-ml polystyrene tubes. The number of cells that migrated into the wells was determined by counting on a FACSCalibur (BD Biosciences). The antagonist activity of INCB3344 on CCR5-mediated chemotaxis was expressed as the total migration minus the background migration.

ERK phosphorylation

WEHI-274.1 cells were aliquoted into microfuge tubes at 5×10^6 cells/sample in 1.0 ml of CCR2 binding buffer and prewarmed to 37°C for 10 min. Compound was added for 5 min before stimulation. The samples were stimulated with mCCL2 (30 nM; R&D Systems) for 1 min. The cells were quickly pelleted, the supernatant was removed, and 100 μl of ice-cold lysis buffer containing 10 mM Tris (pH 7.2), 150 mM NaCl, 1% Triton X-100, 1% deoxycholic acid, 0.1% SDS, 50 μg/ml leupeptin, 50 μg/ml aprotinin, 1 mM sodium vanadate, 50 mM sodium fluoride, and 1 mM PMSF was added. After 10 min on ice, the samples were microfuged at 13,000 rpm for 10 min at 4°C, and the supernatants were collected. For Western analysis, 15 μl of 2× Laemmli sample buffer was added to 15 μl of cell extract, and the samples were boiled for 5 min and loaded onto 10% Tris-Glycine gels (Invitrogen Life Technologies). Following electrophoresis and transfer onto PVDF membrane, the membranes were probed with either a rabbit polyclonal anti-phospo-ERK Ab or rabbit polyclonal anti-ERK to detect total ERK protein (1/1000 dilution; Cell Signaling Technology) followed by a HRP-conjugated goat anti-rabbit IgG Ab (1/2000; Cell Signaling Technology). After washing the blots in PBS + 0.1% Tween 20, chemiluminescent detection reagent (Pierce) was added, the blots exposed to film, and developed.

Selectivity assays against GPCRs

A panel of GPCR binding assays was performed by Cerep. The receptors tested included the following: human adenosine A1, A2A, and A3 receptors; adrenergic receptors α1 (nonselective), α2 (nonselective), β1 (nonselective), 2 (nonselective), and 1; angiotensin II receptor 1 (AT1); bradykinin receptor 2 (B2); cholecystokinin receptor 1 (CCK1); dopamine D1 and D2S receptors; endothelin receptor A (ETA); rat brain GABA receptor; galanin receptor 2 (GAL2); CXCR2; CCR1; histamine receptors H1 and H2; melanocortin receptor 4 (MC4); chicken melatonin receptor 1 (ML1); muscarinic receptors M1, M2, and M3; neurokinin receptors 2 and 3 (NK2, NK3); neuropeptide receptors 1 and 2 (NPY1, NPY2); neurotensin receptor 1 (NT1); opioid receptors d (DOP), k (KOP), and μ (MOP); nociceptin receptor (ORL1); serotonin receptors 5-HT1A, 5-HT2A, 5-HT3, 5-HT5A, 5-HT6, 5-HT7, and rat 5-HT1B; mouse somatostatin receptor (SST); vasoactive intestinal peptide receptor 1 (VIP1); and vasopressin receptor 1 (V1a). All assays were run using recombinant human receptors, except where noted. The full methods and references can be found on the Cerep website (www.cerep.fr). The assays were run at 1 μM INCB3344, and a percentage of inhibition was calculated based on two separate determinations.

Animals

Female BALB/c mice (20 g; Charles River Laboratories) were used for peritonitis and delayed-type hypersensitivity (DTH) studies. C57BL/6 (Charles River Laboratories) were used for the EAE model. Female Lewis rats (Charles River Laboratories) were used for the rat adjuvant arthritis studies. Rodents were allowed water and food ad libitum. Animals were housed in accordance with the Haskell Animal Care and Use Committee (HACUC), and experiments were performed in compliance with the institutional guidelines of HACUC.

Pharmacokinetics

Blood samples were collected at 0, 0.5, 1, 2, 4, 6, 8, 12, and 24 h after dosing using EDTA as the anticoagulant and centrifuged to obtain plasma. INCB3344 and internal standard (INCB3091) were extracted from plasma by liquid-liquid extraction using a 96-well plate format. Briefly, 50 μl of INCB3352 (200 nM), 200 μl of 0.1 M NaHCO3, and 800 μl of methyl t-butyl ether were added to 100 μl of plasma sample in a 96-well plate. The plate was vortexed, centrifuged, and the organic layer transferred into another 96-well plate. The plate was evaporated to dryness, residues were reconstituted with 100 μl of 25% acetonitrile, and 10 μl of sample was injected into liquid chromatography/mass spectrometry for analysis. The chromatographic separation was accomplished using a Zorbax SB-C8 column (3.5 μm, 50 $\times$ 2.1 mm) with a gradient elution. The mobile phase used consisted of 0.1% acetic acid in acetonitrile and 2 mM ammonium acetate. Mobile phase A increased in gradient from 34 to 42% over 5 min at flow rate 300 μl/min. INCB3344 and INCB3091 were detected by positive electrospray using a Sciex API-3000 triple quadruple mass spectrometer. The linear dynamic ranged from 5 to 5000 nM.

Thioglycolate-induced peritonitis

BALB/c mice received injections in the i.p. cavity with 2 ml of fluid thioglycolate medium (VWR). Peritoneal lavages were performed after thioglycolate medium injections, by injecting 5 ml of PBS with 0.1% EDTA into the peritoneal cavity. Cell counts were performed by Coulter Counter (Beckman Coulter). Cytospins were performed to determine differential leukocyte counts. The cells were stained for 3 min with Wright-Giemsa Stain (Sigma-Aldrich) and then rinsed with deionized water for 10 min. Differential counts were calculated based on a total of 100 cells counted per sample in five high-powered fields.

DTH in mice

BALB/c female mice were epicutaneously sensitized with 25 μl of 0.5% hapten (2,4-dinitro-fluorobenzene (DNFB); Sigma-Aldrich) on the shaved skin of their abdomen. Twenty-four hours after the first application, a second application of 25 μl of 0.5% DNFB was applied to the same area as a booster. Five days later, mice were anesthetized, and both of their ears are measured for thickness using an engineer's micrometer. These ear measurements were recorded and used as a baseline. Following recovery from anesthesia, mice received a topical application of 0.2% DNFB (10 μl on the internal pinna and 10 μl on the external pinna) to induce DTH response. Ear swelling is calculated by subtracting the baseline ear thickness of the ear from that following DNFB challenge and is expressed as units of swelling (microns). Ears are either fixed in formalin and paraffin embedded for histopathological analysis or frozen in liquid nitrogen for real-time PCR analysis.

Real-time PCR

Real-time PCR was performed essentially as described (21). Primers and probes designed to specifically detect the murine CCR2 (accession no. NM_009915), CCL2 (accession no. NM_011333), and CD68 (accession no. NM_009853) transcripts were synthesized and purified by Biosearch Technologies. All probes, with the exception of the 18S rRNA probe, were modified at the 5′ end with the reporter dye FAM-aminohexylamidite and at the 3′ end with the black hole quencher BHQ1. The 5′ end of the 18 S rRNA probe was modified with VIC (Applied Biosystems). For detection of murine CCR2 mRNA, primers 5′-AGGGTCACAGGATTAGGAAG GTT and 5′-CGTTCTGGGCACCTGATTTAA and probe 5′-CCACT GCTCATGGATATGTTGAACAATAGAGACC were used. For detection of murine CCL2 mRNA, primers 5′-GCATCTGCCCTAAGGTCTTCA and 5′-GTGGAAAAGGTAGTGGATGCATT and probe 5′- ACCTTT GAATGTGAAGTTGACCCGTAAATCTGAAG were used. For detection of murine CD68 mRNA, primers 5′-AGCTCCCTTGGGCCAAAG and 5′-AAGGTGAACAGCTGGAGAAAGAA and probe 5′-TTCTGCTGTG GAAATGCAAGCA were used. For 18S rRNA, primers 5′-CGGCTAC CACATCCAAGGAA and 5′-GCTGGAATTACCGCGGCT and probe 5′-TGCTGGCACCAGACTTGCCCTC were used. Total RNA was prepared from murine ears using the RNeasy purification system (Qiagen) according to the manufacturer's instructions. cDNA synthesis was performed with the Advantage RT-PCR kit (Clontech Laboratories) according to manufacturer's instructions using random hexamers and 1 μg of DNase I-treated total RNA. For TaqMan-based real-time PCR expression profiling, 25 ng of each cDNA was added to the TaqMan Universal PCR Master Mix along with 900 nM of each primer and 200 nM of probe according to the manufacturer's instructions (Applied Biosystems). Real-time fluorescence monitoring was performed with the ABI Prism 7900 (Applied Biosystems). Relative expression levels of the various transcripts were determined essentially as described (20). Briefly, standard curves were generated for each transcript using a serial dilution of cDNA generated from mouse ear samples isolated from DNFB-sensitized and challenged animals. Relative abundance was then determined by comparing the cycle threshold values for each reaction with this standard curve. Abundance levels calculated from negative control reactions performed in the absence of reverse transcriptase were then subtracted from experimental sample abundance. Input levels of cDNA were normalized to 18 S rRNA levels. All expression measurements were performed in duplicate using two independently generated cDNA samples.

Experimental autoimmune encephalomyelitis

Mice were immunized with 200 μg myelin oligodendrocyte glycoprotein (MOG) 35–55 (BioSource International) emulsified in CFA containing 4 mg/ml *Mycobacterium tuberculosis* (Sigma-Aldrich) s.c. on day 0. In addition, on day 0 and day 2 animals were given 200 ng of pertussis toxin (Calbiochem) i.v. Clinical scoring was based on a scale of 0–5: 0, no signs of disease; 1, flaccid tail; 2, hind limb weakness; 3, hind limb paralysis; 4, forelimb weakness or paralysis; 5, moribund. Dosing of INCB3344 was initiated on day 0 or day 7 and dosed once per day at 100 mg/kg s.c. Spinal cord mononuclear cells were isolated via discontinuous Percoll-gradient (9). Cells were stained using rat anti-mouse F4/80-PE or rat IgG2b-PE (Caltag Laboratories) and quantitated by FACS analysis using 10 ul of Polybeads per sample (Polysciences).

Adjuvant-induced arthritis in rat

Female Lewis rats received injections at the base of the tail with 100 ul of an emulsion of CFA (1 mg of *Mycobacterium butyricum* in IFA) to induce adjuvant arthritis. Rats are monitored daily for the clinical signs of arthritis, which may begin between 10 and 14 days after the injection. Each rat paw was scored using a rating of 0–3 (0, normal; 1, slight redness; 2, redness and swelling; 3, substantial redness and swelling). Ankles were harvested on day 21 and placed in decalcifying solution followed by 10% formalin. Ankles were cut and stained with H&E. Histological analyses were performed on a scale of 0–7 as follows: 0, normal; 1, minimal; 2, mild; 3, moderate; 4, marked; 5, severe; 6, very severe; 7, near destruction of joint for bone resorption or 7, very severe infiltration with severe edema and periarticular tissue expansion for inflammation scoring.

Statistical analysis

Statistical significance of differences between means was analyzed using the paired two-tailed *t* test with significance set at *p* values below 0.05.

Results

In vitro pharmacology of INCB3344

Binding inhibition studies with INCB3344. Characterization of the pharmacological activity of INCB3344 was first evaluated by testing its ability to inhibit CCL2 binding to CCR2 in a whole cell binding assay using a murine monocyte cell line, WEHI-274.1 and ^{125}I-labeled mCCL2 as a tracer. Previous studies showed that mCCL2 binding to the WEHI-274.1 cell line is specific with a K_d of 0.6 nM (data not shown), consistent with the published K_d value of CCL2 binding to recombinant CCR2 (22). The binding IC_{50} of INCB3344 in this assay was determined to be 10 ± 5 nM, and inhibition of >90% binding was observed at a concentration of 90 nM (Fig. 1*a*).

The structural isomer of INCB3344, INCB3090 (19), was also tested in the mCCL2 binding assay. This molecule demonstrated poor CCR2 antagonistic activity with an IC_{50} of >600 nM (Fig. 1*a*), suggesting specific conformational requirements for INCB3344, which enable its interaction with CCR2 and its inhibition of CCR2 binding.

Inhibition of monocyte chemotaxis by INCB3344. A chemotaxis assay using WEHI-274.1 cells was established to evaluate the functional antagonism of murine CCR2 by INCB3344. We first evaluated the dose-response effect of mCCL2 in this assay, which showed a typical bell-shaped curve with maximal activity of CCL2 at 30 nM concentration (data not shown). The chemotaxis inhibitory activity of different concentrations of INCB3344 was evaluated using 30 nM mCCL2 as the agonist. Results from this study indicate that the INCB3344 concentration required for IC_{50} of CCL2-specific migration of WEHI-274.1 cells is 10 ± 6 nM (Fig. 1*b*), similar to its potency in the CCL2 binding assay. In addition and consistent with the weak activity in the binding assay, INCB3090 demonstrated weak CCR2 antagonistic activity in the CCL2 chemotaxis assay with an IC_{50} of >800 nM (Fig. 1*b*). These data suggest that the inhibitory effect of INCB3344 on monocyte migration is pharmacologically related to its CCR2 receptor antagonism.

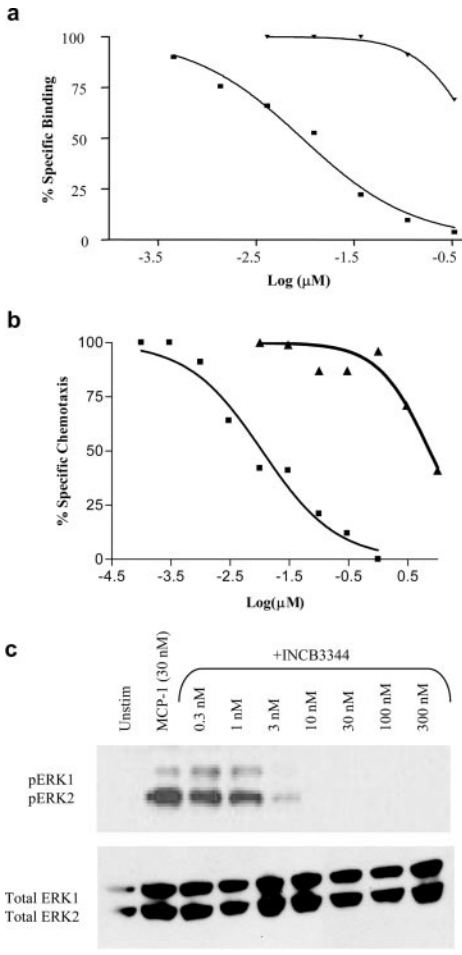

FIGURE 1. Effects of INCB3344 and INCB3090 on binding and functional responses of WEHI-274 cells to CCL2. *a*, Inhibition of CCL2 binding to WEHI cells by INCB3344 (■) but not INCB3090 (▲). *b*, Dose-dependent inhibition of mCCL2-induced chemotaxis of WEHI-274 cells by INCB3344 (■) but not INCB3090 (▲). The IC_{50} of binding inhibition by INCB3344 is 10 nM. *c*, INCB3344 inhibits ERK phosphorylation in response to CCL2 stimulation in WEHI274 cells. IC_{50} value of INCB3344 on ERK phosphorylation is similar to that in chemotaxis assay. A representative Western blot is shown.

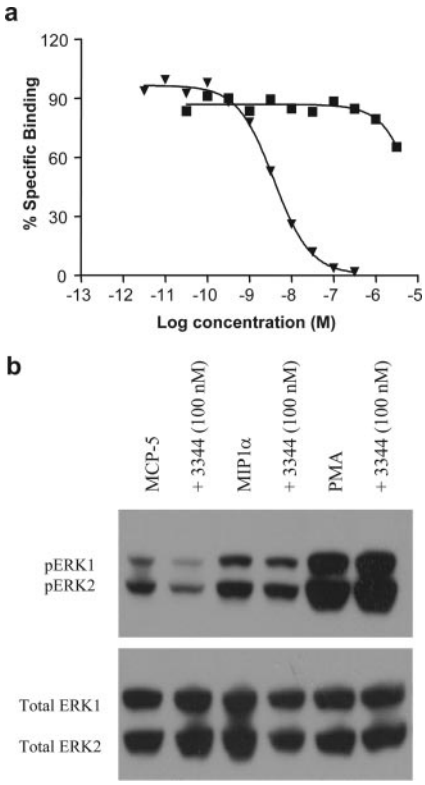

FIGURE 2. Lack of inhibition of INCB3344 on MIP-1β binding or signaling. *a*, INCB3344 (■) or unlabeled MIP-1β (▲), as a positive control, were evaluated in a binding assay using HEK293SFM cells stably transfected with murine CCR5 to determine the cross-reactivity of INCB3344 on murine CCR5. INCB3344 was inactive in this assay at concentrations up to 3 μM. *b*, INCB3344 inhibits ERK phosphorylation in response to MCP-5, a ligand for CCR2, but does not inhibit phosphorylation induced by the CCR1 ligand, MIP-1α, or a nonspecific activator PMA in WEHI-274 cells.

Inhibition of CCR2 signaling by INCB3344. The MAPK signal transduction pathway has been shown to be activated in response to the interaction of CCR2 with ligand, and this pathway is believed to be the key component of the cellular events leading to integrin activation and chemotaxis (23, 24). The effects of INCB3344 on MAPK phosphorylation and activation in response to mCCL2 stimulation were therefore examined. WEHI-274.1 cells were stimulated for 1 min with 30 nM mCCL2 in the presence or absence of various concentrations of INCB3344 (Fig. 1*c*). Cell extracts were prepared and examined by Western blot using an Ab specific for the active phosphorylated form of the MAPK family members, ERK1 and ERK2. INCB3344 did not induce

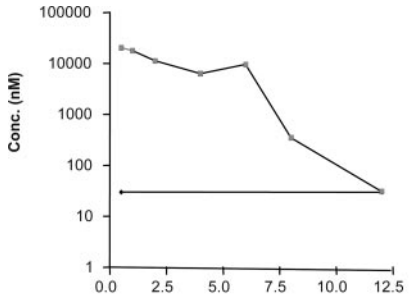

Dose	Average Blood Trough Conc.	Calculated % Inhibition at Trough*
30 mg/kg	30 nM	~40%
50 mg/kg	150 nM	~75%
100 mg/kg	1000 - 3000 nM	>90 %

FIGURE 3. Pharmacokinetics of INCB3344 after a single oral dose of 30 mg/kg. The 12-h trough plasma concentrations of three doses of INCB3344 and corresponding predicted inhibition of CCR2 are shown.

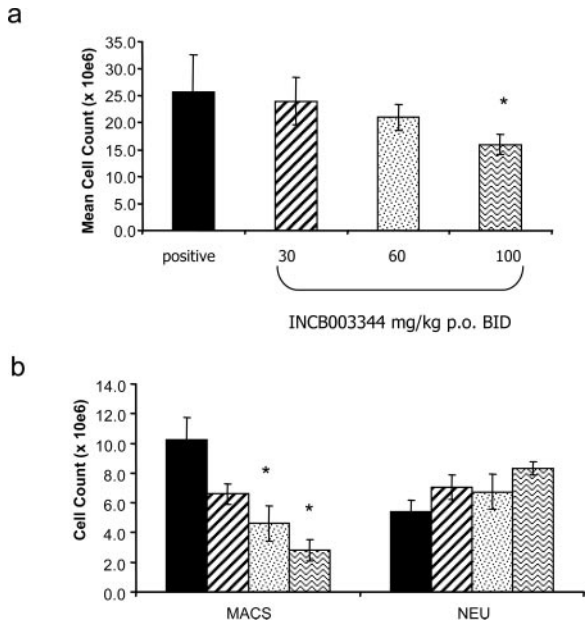

FIGURE 4. Inhibition of macrophage influx by INCB3344 in the thioglycolate-induced peritonitis model. *a*, Effect of INCB3344 treatment on the total cell number in the lavage fluid following thioglycolate injection. Vehicle (■) or different doses of INCB3344, 30 mg/kg BID (▧), 60 mg/kg BID (▨), or 100 mg/kg BID (▩) were evaluated in this model. *b*, Specific effects of INCB3344 on macrophages vs neutrophils.

ERK phosphorylation when added by itself at 10 μM, indicating a lack of agonist activity. INCB3344 blocked ERK phosphorylation in response to mCCL2 with an IC_{50} value of 3–10 nM, consistent with its potency in blocking chemotaxis. INCB3344 had no effect on total ERK levels (Fig. 1*c*).

Selectivity of INCB3344. Selectivity of INCB3344 was evaluated against a panel of GPCRs including several human chemokine receptors using radioligand binding assays. Results from these studies demonstrate at least 100-fold selectivity of INCB3344 against all of the receptors tested (data not shown).

Because CCR1 and CCR5 are most homologous to CCR2, we performed further analysis of INCB3344 activity against these two murine receptors. To determine the effect of INCB3344 on MIP-β binding to murine CCR5, a HEK293SFM cell line was established that stably expresses murine CCR5. In the competition binding assay, using human ^{125}I-MIP-1β as radioligand and the mouse CCR5 transfectants as the source of the receptor, mouse MIP-1β potently inhibited the radioligand binding to the receptor ($IC_{50} \approx$ 4.5 nM). In contrast, INCB3344 demonstrated <50% inhibitory activity at concentrations >3 μM (Fig. 2*a*), indicating that this molecule does not antagonize the mouse CCR5 receptor. INCB3090 also lacks activity in this assay when evaluated at concentrations up to 3 μM (data not shown). To evaluate the functional effects of INCB3344 on mouse CCR5, a chemotaxis assay was performed using murine T cells with MIP-1β as the chemoattractant. The IC_{50} of INCB3344 in this assay was >3 μM, again indicating that the compound does not antagonize mouse CCR5 (data not shown). The selectivity of INCB3344 and INCB3090 were also determined against murine CCR1. Murine MIP-1α (100 nM) was used as the chemoattractant for the WEHI-274.1 cells (which express CCR1) in the chemotaxis assay. The IC_{50} for both compounds were >1 μM, indicating selectivity against CCR1 (data not shown). In addition, selectivity was tested for migration of WEHI-274.1 cells to C5a, FMLP, and RANTES in the presence of INCB3344. There was no impact on the ability of these cells to migrate to these potent chemoattractants in the presence of INCB3344, further confirming the CCR2 selectivity of this compound (data not shown).

Finally, we evaluated the effects of INCB3344 on ERK phosphorylation induced by another known ligand specific for CCR2, MCP-5, and a CCR1 ligand, MIP1α, to determine potentially weak cross-reactivity to CCR1 that cannot be measured in binding and chemotaxis assays. The effect of INCB3344 on PMA-induced ERK phosphorylation was also measured to exclude nonreceptor-mediated effects on this signaling event (Fig. 2*b*). Results from these studies clearly demonstrate that INCB3344 inhibits ERK phosphorylation selectively induced by CCR2 ligands but not by other mechanisms.

In vivo pharmacology of INCB3344

Pharmacokinetics of INCB3344. The pharmacokinetic profile of INCB3344 was evaluated in mice following oral administration at a dose of 30 mg/kg. INCB3344 exhibited a time-concentration relationship consistent with two-compartment distribution (Fig. 3). Based on the pharmacokinetic profile of INCB3344, in vitro chemotaxis inhibitory potency, and free fraction of INCB3344 in mouse plasma (15% fu), dosing regimens that targeted different levels of CCR2 inhibition at trough were designed for evaluation in animal models. At 30, 50, and 100 mg/kg oral doses, predicted inhibition of CCR2-mediated signaling at 12-h trough plasma concentrations were 40, 75, and >90%, respectively (Fig. 3).

Inhibition of macrophage influx by INCB3344. Because multiple studies using CCR2 knockout mice have demonstrated a selective reduction of monocyte influx in the thioglycolate-induced peritonitis model (5–7), we used this model as a simple in vivo system to evaluate the pharmacodynamics and specificity of INCB3344, before extensive and longer-term in vivo studies.

Groups of mice received i.p. injection of thioglycolate followed by oral administration of vehicle or different doses of INCB3344 (30, 60, or 100 mg/kg BID). Mice were sacrificed 48 h later, and peritoneal lavages were obtained for cell influx analysis. At this time point, in control mice, the cellular component of peritoneal lavage consisted predominantly of macrophages and neutrophils with very few lymphocytes present. Treatment of mice with INCB3344 resulted in a dose-dependent reduction of total cell number in the lavage fluid, but the differences reached statistical

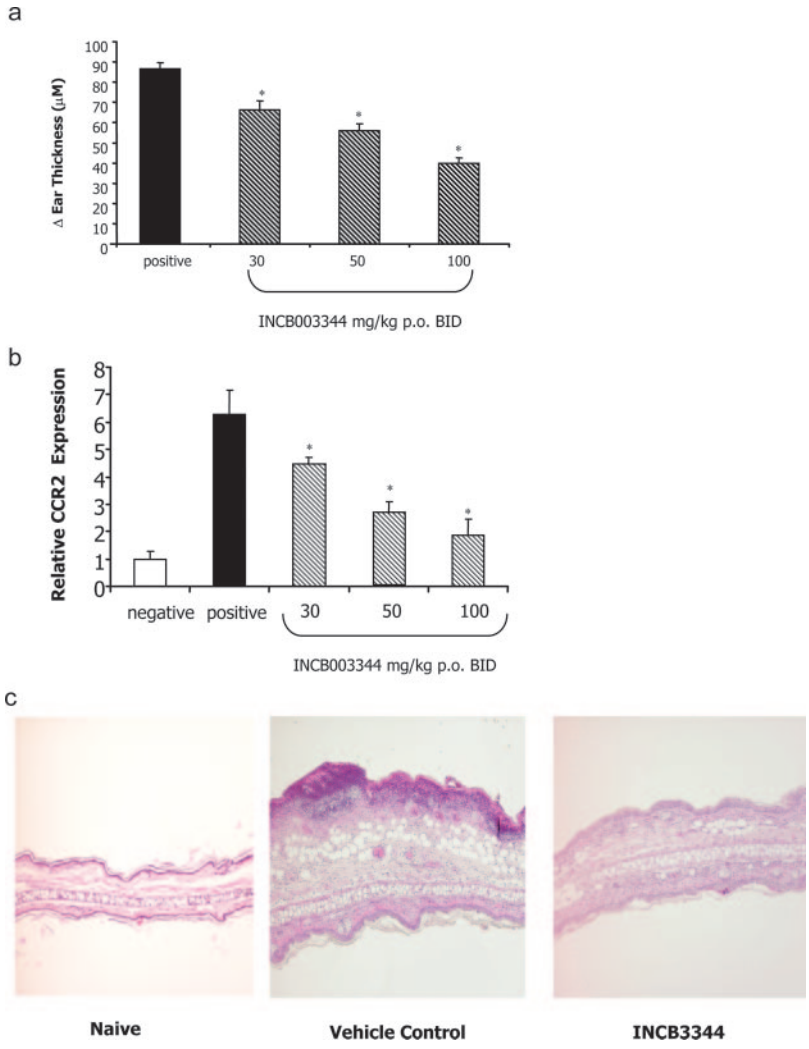

FIGURE 5. INCB3344 inhibits DTH response in mice. *a*, INCB3344 inhibition of ear swelling after DNFB challenge is dose responsive. *b*, Expression of CCR2 mRNA is significantly decreased by INCB3344 treatment. *c*, H&E staining of 5-μm ear sections illustrating the significant decrease in inflammatory cell infiltrate following treatment with INCB3344. *, $p < 0.02$ (two-tailed *t* test).

significance (Fig. 4*a*) ($p < 0.005$) only at the highest dose tested. Analysis of the differential leukocyte counts by morphological evaluation of cytospins from the lavage fluid demonstrated a dose-dependent suppression of monocyte influx (36% at 30 mg/kg, 55% at 60 mg/kg, and 73% at 100 mg/kg) (Fig. 4*b*) with 60 and 100 mg/kg doses showing statistically significant effects ($p < 0.02$) with no statistically significant effects on the total numbers of lymphocytes, a minor fraction of the total cell infiltrate in this model.

To exclude potential nonspecific effects of INCB3344 on cell migration, we also examined the effect of INCB3344 administration on the non-CCR2-bearing neutrophil fraction of the peritoneal lavage. Results, shown in Fig. 4*b*, demonstrate that INCB3344 did not impact peritoneal influx of neutrophils at any of the doses tested. We also examined the effects of INCB3344 administration on the eosinophil fraction of the lavage fluid and did not observe any differences between vehicle and INCB3344 groups (data not shown). These results indicate that the effect of INCB3344 in this model is specific to macrophages.

We further evaluated the possibility of non-CCR2-mediated effects of INCB3344 contributing to its inhibition in the thioglycolate peritonitis model by using $CCR2^{-/-}$ mice. It has been previously demonstrated that there is an incomplete (~70%) inhibition of macrophage influx in $CCR2^{-/-}$ mice with this model. If the effect of INCB3344 is solely mediated through CCR2, then the treatment of $CCR2^{-/-}$ mice with this molecule should not impact the remaining peritoneal macrophage influx. Indeed, when groups of $CCR2^{-/-}$ mice were subjected to thioglycolate peritonitis following INCB3344 treatment (100 mg/kg), no further reduction of peritoneal macrophage influx was observed with INCB3344 beyond what occurs due to the absence of the *CCR2* gene (data not shown).

Suppression of DTH response by INCB3344. Given that INCB3344 inhibits macrophage influx in an in vivo model in a manner similar to that observed in the $CCR2^{-/-}$ mice, and given that it has a favorable pharmacokinetic profile allowing dose-dependent inhibition of CCR2 in vivo, we sought to assess the activity of the molecule in a more complex model of cell-mediated immunity. One such model is the DTH reaction (25). This well-characterized model consists of a sensitization phase (immune education phase), and a challenge phase (inflammatory phase). A positive DTH reaction results in the influx of Ag-specific T cells as well as other inflammatory cells, including macrophages, leading to inflammation of the challenged tissue. We performed this model in mice using the ear as the challenge site and used ear thickness change as a gross measure of the degree of inflammation. Additionally, a more quantitative and specific measurement of macrophage influx in this model was obtained by using quantitative real-time PCR (qPCR) to measure the expression of CCR2 and other relevant inflammation-related marker genes from ear cDNA samples.

To determine the effect of INCB3344 in the murine DTH reaction, groups of mice ($n = 6$–8) were administered either vehicle or INCB3344 at varying doses orally twice a day (30, 50, and 100

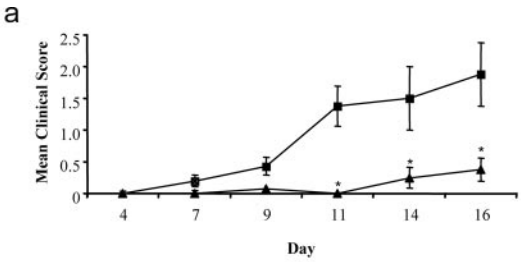

Group	Incidence	CDI[a]
Vehicle	7/8 (87.5%)	9.6 ± 4
INCB3344(100mg/kg sc QD)	2/8 (25%)	1 ± 1.3

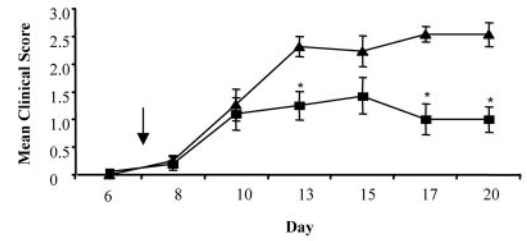

Group	Incidence	CDI[a]
Vehicle	13/13(100%)	20 ± 13.1
INCB3344(100mg/kg sc QD)	9/14(64%)	11.3 ± 6.2

[a] cumulative disease index (CDI) is the mean of the sum of the daily clinical scores observed for the duration of the study. Shown are the mean SD for each group.

FIGURE 6. INCB3344 is efficacious in the MOG-induced model of mouse EAE. Treatment of mice orally with INCB3344 100 mg/kg s.c QD (▲) *a*, Dosing from the time of immunization results in significant suppression of the clinical signs of disease as compared with vehicle-treated animals (■) *b*, Dosing was initiated 7 days postimmunization. The data are expressed as the mean clinical disease score for all mice in each group as a function of days after immunization. Mean clinical disease severity was significantly decreased in INCB3344-treated animals (n = $p < 0.05$, two-tailed *t* test).

mg/kg), starting at the time of ear challenge with DNFB (inflammatory phase only). Ear thickness was measured, as a clinical measure of ear inflammation, 48 h after ear challenge. Mice were then sacrificed, and both ears were collected for analysis of CCR2 expression by qPCR and for histological evaluation of inflammation. INCB3344 treatment resulted in a dose-dependent suppression of ear swelling (Fig. 5*a*). The percentages of inhibition compared with the vehicle-treated group were 23, 35, and 54% in 30, 50, and 100 mg/kg BID dose groups, respectively ($p < 0.01$). Using qPCR analysis of CCR2 mRNA (a gene that is predominantly expressed by monocytes/macrophages), we evaluated the impact of INCB3344 treatment on tissue macrophage burden (Fig. 5*b*). At doses of 30, 50, and 100 mg/kg BID, INCB3344 treatment resulted in 34, 69, and 84% inhibition of CCR2 mRNA (normalized to 18S RNA), respectively. This correlated with a significant decrease in CD68, a macrophage surface marker, as well CD4, a marker for helper T cells primarily found in the infiltrate in this model. Histological analyses also demonstrated a decrease in the inflammatory cell component in the dermis of the ears following INCB3344 treatment (Fig. 5*c*). To exclude the possibility that the INCB3344 activity in the murine DTH model was due to potential non-CCR2-mediated effects, the pharmacologically inactive INCB003090 was tested in DTH. Administration of INCB3090 did not result in appreciable inhibition of macrophage influx as determined by qPCR analysis of CCR2 mRNA or inhibition of ear swelling (data not shown).

INCB3344 is protective in the mouse EAE model. It has previously been reported that CCL2 and CCR2 knockout mice are resistant to the development of MOG-induced EAE (9, 10, 18). A similar model system has been used to evaluate the role of other chemokine receptors, CCR1 and CCR5, which are also present on monocytes. Although CCR1 gene deletion resulted in a lower incidence of disease (26), the effect was not nearly as profound as that observed in CCR2 or CCL2 knockout mice. Mice with the CCR5 gene deletion did not show any impact on the development of EAE (27). Given the demonstrated role of CCR2 in this well-characterized model, we chose mouse EAE as a disease model system to further evaluate the efficacy of INCB3344.

Starting from the day of immunization, mice received vehicle or INCB3344 (100 mg/kg QD) by s.c. administration and were monitored for the development of clinical signs of disease. The s.c. dosing regimen was used in this study because it allows once daily dosing. At this dose, in vivo CCR2 inhibition is ~75% at trough (24 h postdose). The mean clinical scores of mice treated with INCB3344 were significantly lower ($p < 0.05$) than those receiving vehicle (Fig. 6*a*), with a significant difference in disease incidence (vehicle 87.5% vs INCB3344 25%). Treatment with INCB3344 also resulted in a 50% decrease in the number of macrophages (F4/80 positive) isolated from the spinal cords (vehicle 5.8×10^5 vs INCB3344 2.4×10^5). Although prophylactic dosing replicates the data in the CCR2 knockout, we also show antagonism of CCR2 in a therapeutic dosing regimen. As shown in Fig. 6*b*, animals that received their first dose of INCB3344 7 days after immunization still showed significant inhibition of disease as manifested by suppression of the apparent disease incidence (vehicle 100% vs INCB3344 64%) as well as severity (maximum mean clinical score vehicle 2.57 ± 0.78 vs INCB3344 1.43 ± 1.22). Dosing was initiated on day 7 when histological evidence of disease is present but few animals are presenting clinical signs (28). The data clearly show that CCR2 antagonism therapeutically can halt the progression of EAE.

INCB3344 is efficacious in the rat adjuvant arthritis model. INCB3344 was also evaluated therapeutically in the rat adjuvant arthritis model by initiation of dosing at day 9 after adjuvant treatment. This time point correlates to a time at which macrophages have already begun to infiltrate into the joint (29). Significant inhibition of the severity of disease was achieved at 100 mg/kg PO

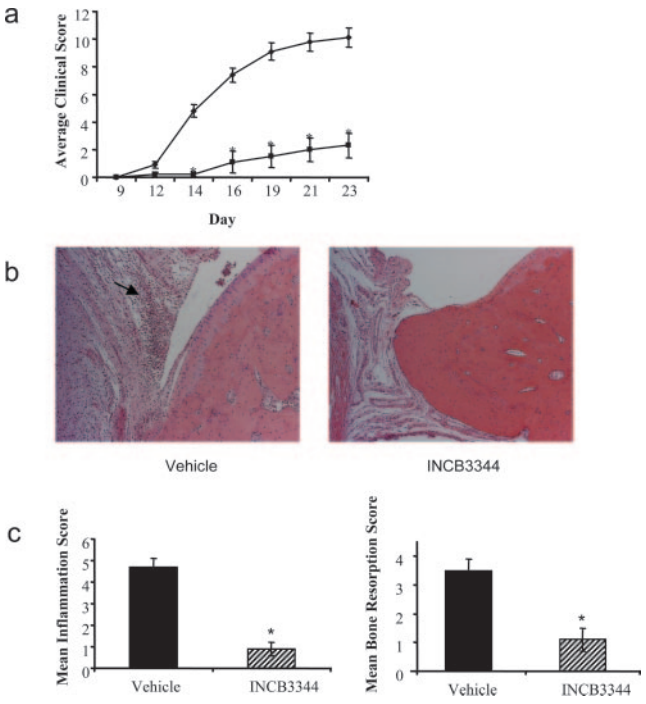

FIGURE 7. INCB3344 is efficacious in rat AIA. Treatment of rats with INCB3344 100 mg/kg BID s.c. from day 9 postimmunization resulted in significant inhibition of clinical and histological disease. *a*, Clinical score: each limb graded on a scale of 0–3, giving a maximum score of 12 per mouse ($n = 10$/group). Histological analyses of ankles. *b*, H&E comparison of ankles from vehicle- and INCB3344-treated animals (arrow indicates area of severe synovitis. *c*, Mean inflammation score and mean bone resorption score. Scored on a scale of 0–7, with 0 = normal and 7 = most severe. *, $p < 0.02$ (two-tailed *t* test).

BID ($p < 0.001$) (Fig. 7*a*). In the rat, this dosing scheme provides an IC_{50} at trough of ~70%. Histological evaluation (Fig. 7*b*) showed significant inhibition of inflammation in the joints of these animals (82% inhibition) as well as significant inhibition of bone resorption (64% inhibition) (Fig. 7*c*).

Discussion

This report is the first description of the pharmacological characterization of a novel, potent, and selective small molecule inhibitor of mouse CCR2. Multiple lines of experimental evidence, derived from radioligand binding and functional assays that are presented in this report strongly support that INCB3344 is a selective and potent antagonist of mouse CCR2. The inactivity of the *cis*-isomer, INCB3090, further establishes the requirement for the molecule to bind and antagonize CCR2. Several chemically distinct series of CCR2 antagonists have been reported in the literature including cinnamides (30), the spiropiperidines (31), and a series of anilide derivatives with a quaternary ammonium moiety (e.g.TAK-779). Many of these molecules lack selectivity as well as the physicochemical and pharmacokinetic profiles to be useful pharmacological tools. More importantly, they also lack rodent cross-reactivity, making pharmacological evaluation of these molecules impossible (32). In this regard, INCB3344 is a small molecule antagonist that overcomes many of the obstacles faced by earlier generation antagonists of CCR2.

The identification of INCB3344 as a rodent-active CCR2 antagonist and the data confirming the knockout phenotype in classical models of macrophage trafficking allows us to better understand the role of macrophages in the development and maintenance of the inflammatory response. The effect of INCB3344 on monocyte infiltration in the thioglycolate-induced peritonitis model are in line with reported data in $CCR2^{-/-}$ mice (5–7), suggesting that pharmacological blockade of CCR2 in normal animals achieves a similar degree of inhibition to gene deletion. Results in this model also show that the observed inhibition of in vivo macrophage influx in this model is consistent with the inhibition predicted from plasma-free drug concentrations and the in vitro chemotaxis potency of INCB3344. The lack of effect on neutrophils in wild-type mice as well as the lack of additional effects on macrophage influx in $CCR2^{-/-}$ mice further supports the hypothesis that the in vivo effects of INCB3344 are mediated through CCR2.

Although DTH studies using CCR2 knockout mice have not been reported in the literature, one published study (8) evaluated the DTH response in CCL2 knockout mice. Our results on monocyte influx in the mouse DTH model are similar to the reported reduction in the number of F4/80-positive macrophages in the ears of $CCL2^{-/-}$ mice undergoing the DTH reaction, although the antagonist was only dosed during the inflammatory phase of the model. INCB3344 treatment also resulted in a concomitant reduction in ear swelling and in the histological signs of inflammation, whereas the previous study with $CCL2^{-/-}$ mice did not have a significant impact on ear swelling. Differences between the published data on the CCL2 knockout and our results may be due to the fact that CCR2 antagonism inhibits binding to multiple members of the MCP family including MCP-2, -3, -4, and -5, whereas CCL2 (MCP-1) gene deletion will only impact a part of the CCR2-mediated biological effects. Another interesting observation from this study is that the blockade of CCR2 in the DTH model appears to have suppressed the overall inflammatory burden of the ears, not just macrophage influx. It is well known that macrophages are capable of producing a number of cytokines and chemotactic factors at sites of inflammation. Based on the results from the DTH studies presented here, it is tempting to speculate that macrophages, in general, and the CCL2/CCR2 pathway, in particular, play an orchestrating role in regulating the cellular immune response in the DTH reaction.

In addition to using mice with targeted disruption of CCR2 and CCL2, several other approaches have been undertaken to understand the potential utility of CCR2 antagonism in inflammatory diseases. These approaches include the use of a protein antagonist of CCR2, generated by deletion of the first 7 aas of CCL2 (33), DNA vaccine using CCL2 DNA (34–36), and Abs to CCR2 and CCL2 (37–39). Although most of these studies confirm the phenotype of knockout mice, they suffer from several issues that preclude a direct extrapolation of the data to a small molecule drug as well as a thorough understanding of the pharmacokinetic/pharmacodynamic relationship of CCR2 antagonism that a small molecule approach affords. With the DNA vaccination approach, it is not possible to precisely control the level of neutralization of the receptor, because multiple Abs with different titers and affinities are generated following DNA vaccination. Anti-CCR2 Abs used in mouse models have been recently shown to deplete circulating monocytes in mice (40) and, hence, are likely to have biological effects that would be qualitatively and quantitatively different from a classic receptor antagonist. Peptide antagonists, in contrast, would have very different tissue distribution profiles from small molecule antagonists. Our data demonstrating efficacy following therapeutic dosing of INCB3344 in the rat AIA model of arthritis is of particular relevance in light of the recent reports showing that, in the collagen-induced arthritis model, disease is actually exacerbated in the CCR2 knockout or when CCR2 is blocked with Abs (37, 41). Although these differences could be due to differences in the models, we have recently shown that INCB3344 also does not exacerbate disease and is in fact efficacious when dosed therapeutically in the collagen-induced arthritis model (C. Brodmerkel and

K. Vaddi, manuscript in preparation). These data further highlight the utility of testing small molecule antagonists in disease models for target validation.

Many well-established anti-inflammatory therapies, including corticosteroids and TNF antagonists, impact leukocyte trafficking indirectly by preventing the up-regulation of adhesion molecules and chemokines. Although it remains to be seen whether blockade of CCR2 can result in strong suppression of tissue trafficking of monocyte in humans, data from the CCR2 knockout mice as well as studies presented in this report with INCB3344 in the mouse EAE model and rat AIA model provide a strong rationale for the clinical evaluation of CCR2 antagonists in multiple sclerosis and RA, among other chronic inflammatory conditions. With a number of oral antagonists of CCR2 undergoing preclinical and clinical evaluations, we believe that a small molecule antagonist such as INCB3344 will be a very instructive tool to understand the potential as well as limitations of therapies targeting CCR2.

Disclosures

C. M. Brodmerkel, R. Huber, M. Covington, S. Diamond, L. Hall, R. Collins, L. Leffet, K. Gallagher, P. Feldman, P. Collier, M. Stow, X. Gu, F. Baribaud, N. Shin, B. Thomas, T. Burn, G. Hollis, S. Yeleswaram, K. Solomon, S. Friedman, A. Wang, C. B. Xue, R. C. Newton, P. Scherle, and K. Vaddi are employees of, and have stock options with, Incyte Corporation.

References

1. Kinne, R. W., R. Brauer, B. Stuhlmuller, E. Palombo-Kinne, and G. Burmester. 2000. Macrophages in rheumatoid arthritis. *Arthritis Res.* 2: 189–202.
2. Barrera, P., A. Blom, P. L. van Lent, L. van Bloois, J. H. Beijnen, N. van Rooiken, M. C. de Waal Malefijt, L. B. van de Putte, and W. B. van den Berg. 2000. Synovial macrophage depletion with clodronate-containing liposomes in rheumatoid arthritis. *Arthritis Rheum.* 43: 1951–1959.
3. Smeets, T. J. M., M. C. Kraan, M. E. van Loon, and P.-P. Tak. 2003. Tumor necrosis factor α blockade reduces the synovial cell infiltrate early after initiation of treatment, but apparently not by induction of apoptosis in synovial tissue. *Arthritis Rheum.* 48: 2155–2162.
4. Power, C. A., and A. E. Proudfoot. 2001. The chemokine system: novel broad-spectrum therapeutic targets. *Curr. Opin. Pharmacol.* 1: 417–424.
5. Boring, L., J. Gosling, S. W. Chensue, S. L. Kunkel, R. V. Farese, Jr., H. E. Broxmeyer, and I. F. Charo. 1997. Impaired monocyte migration and reduced type 1 (Th1) cytokine responses in C-C chemokine receptor 2 knockout mice. *J. Clin. Invest.* 100: 2552–2561.
6. Kurihara, T., G. Warr, J. Loy, and R. Bravo. 1997. Defects in macrophage recruitment and host defense in mice lacking the CCR2 chemokine receptor. *J. Exp. Med.* 186: 1757–1762.
7. Kuziel, W. A., S. J. Morgan, T. C. Dawson, S. Griffin, O. Smithies, K. Ley, and N. Maeda. 1997. Severe reduction in leukocyte adhesion and monocyte extravasation in mice deficient in CC chemokine receptor 2. *Proc. Natl. Acad. Sci. USA* 94: 12053–12058.
8. Lu, B., B. J. Rutledge, L. Gu, J. Fiorillo, N. W. Lukacs, S. L. Kunkel, R. North, C. Gerard, and B. J. Rollins. 1998. Abnormalities in monocyte recruitment and cytokine expression in monocyte chemoattractant protein-1-deficient mice. *J. Exp. Med.* 187: 601–608.
9. Fife, B. T., G. B. Huffnagle, W. A. Kuziel, and W. J. Karpus. 2000. CC chemokine receptor 2 is critical for induction of experimental autoimmune encephalomyelitis. *J. Exp. Med.* 192: 899–905.
10. Huang, D., J. Wang, O. Kivisakk, B. J. Rollins, and R. M. Ransohoff. 2001. Absence of monocyte chemoattractant protein 1 in mice leads to decreased local macrophage recruitment and antigen-specific T helper cell type 1 immune response in experimental autoimmune encephalomyelitis. *J. Exp. Med.* 193: 713–726.
11. Abbadie, C., J. A. Lindia, A. M. Cumiskey, L. B. Peterson, J. S. Mudgett, E. K. Bayne, J. A. DeMartino, D. E. MacIntyre, and M. J. Forrest. 2003. Impaired neuropathic pain responses in mice lacking the chemokine receptor CCR2. *Proc. Natl. Acad Sci. USA* 100: 7947–7952.
12. Boring, L., J. Gosling, M. Cleary, and I. F. Charo. 1998. Decreased lesion formation in $CCR2^{-/-}$ mice reveals a role for chemokines in the initiation of atherosclerosis. *Nature* 394: 894–897.
13. Gu, L., Y. Okada, S. K. Clinton, C. Gerard, G. K. Sukhova, P. Libby, and B. J. Rollins. 1998. Absence of monocyte chemoattractant protein-1 reduces atherosclerosis in low density lipoprotein receptor-deficient mice. *Mol. Cell* 2: 275–281.
14. Gong, J., and I. Clark-Lewis. 1995. Antagonists of monocyte chemoattractant protein-1 identified by modification of functionally critical NH_2-terminal residues. *J. Exp. Med.* 181: 631–640.
15. Kitamoto, S., and K. Egashira. 2003. Anti-monocyte chemoattractant protein-1 gene therapy for cardiovascular diseases. *Expert Rev. Cardiovasc. Ther.* 1: 393–400.
16. Hasegawa, H., M. Kohno, M. Sasaki, A. Inoue, M. R. Ito, M. Terada, and K. Hieshum. 2003. Antagonist of monocyte chemoattractant protein-1 ameliorates the initiation and progression of lupus nephritis and renal vasculitis in MRL/lpr mice. *Arthritis Rheum.* 48: 2555–2566.
17. Gao, Z., and W. A. Metz. 2003. Unraveling the chemistry of chemokine receptor ligands. *Chem. Rev.* 103: 3733–3752.
18. Izikson, L., R. S. Klein, I. F. Charo, H. L. Weiner, and A. D. Luster. 2000. Resistance to experimental autoimmune encephalomyelitis in mice lacking the CC chemokine receptor (CCR)2. *J. Exp. Med.* 192: 1075–1080.
19. Xue, C., B. Metcalf, H. Feng, G. Cao, T. Huang, C. Zheng, D. J. Robinson, and A. Han. 3-Aminopyrrolidine derivatives as modulators of chemokine receptors. U.S. Patent Application WO2004/050024. Incyte Corporation. Filed November 2003. Published June 2004.
20. Rollins, B., A. Walz, and M. Baggiolini. 1991. Recombinant human MCP-1/JE induces chemotaxis, calcium flux and the respiratory burst in human monocytes. *Blood* 78: 1112–1116.
21. Gibson, U. E., C. A. Heid, and P. M. Williams. 1996. A novel method for real time quantitative RT-PCR. *Genome Res.* 6: 995–1001.
22. Ernst, C., Y. Zhang, P. Hancock, B. Rutledge, C. Corless, and B. Rollins. 1994. Biochemical and biologic characterization of murine monocyte chemoattractant protein-1: identification of two functional domains. *J. Immunol.* 152: 3541–3549.
23. Wain, J., J. Kirby, and S. Ali. 2002. Examination of mitogen-activated protein kinase and phosphoinositide 3-kinase activation by monocyte chemoattractant proteins-1, -2, -3 and -4. *Clin. Exp. Immunol.* 127: 436–444.
24. Ashida, N., H. Arai, M. Yamasaki, and T. Kita. 2001. Distinct signaling pathways for MCP-1 dependent integrin activation and chemotaxis. *J. Biol. Chem.* 276: 16555–16560.
25. Black, C. A. 1999. Delayed type hypersensitivity: current theories with an historic perspective. *Dermatol. Online J.* 5: 7.
26. Rottman, J. B., A. J. Slavin, R. Silva, H. Weiner, C. G. Gerard, and W. W. Hancock. 2000. Leukocyte recruitment during onset of experimental allergic encephalomyelitis is CCR1 dependent. *Eur. J. Immunol.* 30: 2372–2377.
27. Tran, E. H., W. A. Kuziel, and T. Owens. 2000. Induction of experimental autoimmune encephalomyelitis in C57BL/6 mice deficient in either the chemokine macrophage inflammatory protein-1α or its CCR5 receptor. *Eur. J. Immunol.* 30: 1410–1415.
28. Polman, C. H., C. D. Dijkstra, T. Sminia, and J.C. Koetsier. 1986. Immunohistological analysis of macrophages in the central nervous system of Lewis rats with acute experimental allergic encephalomyelitis. *J. Neuroimmunol.* 11: 215–222.
29. Halloran, M. M., Z. Szekanecz, N. Barquin, G. K. Haines, and A. E. Koch. 1996. Cellular adhesion molecules in rat adjuvant arthritis. *Arthritis Rheum.* 39: 810–819.
30. Forbes, I. T., D. G. Cooper, E. K. Dodds, D. M. B. Hickey, R. J. Ife, M. Meeson, T. Berkhout, J. Gohil, and K. Moores. 2000. CCR2B receptor antagonists: conversion of a weak HTS hit to a potent lead compound. *Bioorg. Med. Chem. Lett.* 10: 1803–1806.
31. Mirzadegan, T., F. Diehl, B. Ebi, S. Bhakta, I. Polsky, D. McCarley, M. Mulkins, G. S. Weatherhead, J. Lapierre, J. Dankwardt, et al. 2000. Identification of the binding site for a novel class of CCR2B chemokine receptor antagonists. *J. Biol. Chem.* 275: 25562–25571.
32. Berkhout, T. A., F. E. Blaney, A. M. Bridges, D. G. Cooper, I. T. Forbes, A. D. Grible, P. H. E. Groot, A. Hardy, R. J. Ife, R. Kaur, et al. 2003. CCR2: characterization of the antagonist binding site from a combined receptor modeling/mutagenesis approach. *J. Med. Chem.* 46: 4070–4086.
33. Gong, J.-H., L. G. Ratkay, J. D. Waterfield, and I. Clark-Lewis. 1997. An Antagonist of MCP-1 inhibits arthritis in the MRL-lpr mouse model. *J. Exp. Med.* 186: 131–137.
34. Youssef, S., G. Maor, G. Wildbaum, N. Grabie, A. Gour-Lavie, and N. Karin. 2000. C-C chemokine-encoding DNA vaccines enhance breakdown of tolerance to their gene products and treat ongoing adjuvant arthritis. *J. Clin. Invest.* 106: 361–371.
35. Youssef, S., G. Wildbaum, G. Maor, N. Lanir, A. Gour-Lavie, N. Grabie, and N. Karin. 1998. Long-lasting protective immunity to experimental autoimmune encephalomyelitis following vaccination with naked DNA encoding C-C chemokines. *J. Immunol.* 161: 3870–3879.
36. Ni, W., K. Egashira, S. Kitamoto, C. Kataoka, M. Koyanagi, S. Inoue, K. Imaizumi, C. Akiyama, K. Nishida, and A. Takeshita. 2001. New anti-monocyte chemoattractant protein-1 gene therapy attenuates atherosclerosis in apolipoprotein E-knockout mice. *Circulation* 103: 2096–2101.
37. Bruhl, H., J. Cihak, M. Schneider, J. Plachy, T. Rupp, I. Wenzel, M. Shakarami, S. Milz, J. Ellwart, M. Stangassinger, et al. 2004. Dual role of CCR2 during initiation and progression of collagen-induced arthritis: evidence for regulatory activity of $CCR2^{+}$ T cells. *J. Immunol.* 172: 890–898.
38. Ogata, H., M. Takeya, T. Yoshimura, K. Takagi, and K. Takahashi. 1997. The role of monocyte chemoattractant protein-1 (MCP-1) in the pathogenesis of collagen-induced arthritis in rats. *J. Pathol.* 182: 106–114.
39. Kennedy, K. J., R. M. Strieter, S. L. Kunkel, N. W. Lukacs, and W. J. Karpus. 1998. Acute and relapsing experimental autoimmune encephalomyelitis are regulated by differential expression of the CC chemokines macrophage inflammatory protein-1α and monocyte chemotactic protein-1. *J. Neuroimmunol.* 92: 98–108.
40. Kishimoto, T. 2004. Mechanistic insights into the biology of CCR2/MCP-1 obtained through the development of anti-CCR2 therapeutic antibodies. In *Chemotactic Cytokine Gordon Research Conference, September 19–24*. Aussois, France.
41. Quinones, M. P., S. K. Ahuja, F. Jimenez, J. Schaefer, E. Garavito, A. Rao, G. Chenaux, R. L. Reddick, W. A. Kuziel, and S. S. Ahuja. 2004. Experimental arthritis in CC chemokine receptor 2-null mice closely mimics severe human rheumatoid arthritis. *J. Clin. Invest.* 113: 856–866.